



# Experimental investigations about the influence of oil lubricant between teeth on the gear rattle phenomenon

Riccardo Russo\*, Renato Brancati, Ernesto Rocca

*Dipartimento di Ingegneria Meccanica per l'Energetica, Università di Napoli "Federico II", via Claudio 21, 80125 Napoli, Italy*

Received 12 February 2008; received in revised form 23 September 2008; accepted 8 October 2008

Handling Editor: C.L. Morfey

Available online 20 November 2008

---

## Abstract

The article describes an experimental investigation into the “gear rattle” phenomenon in automotive manual transmissions with a special focus on the influence that lubricant oil may have in reducing this undesirable event.

The experimental analysis has been conducted in order to validate a theoretical model developed by the authors that accounts for the presence of oil between the meshing gear teeth of unloaded gear pairs during the no-contact phase.

An original measurement technique has been adopted for the tests that consist of the acquisition of the angular relative motion of a gear pair by two high resolution encoders. The experimental test rig designed for this analysis offers the possibility of varying the distance between the wheel axes so that the influence of the backlash variation on the rattle phenomenon can be investigated.

The paper presents the results of a series of experiments conducted on helical gear pairs from an automotive gear box in the “idle gear rattle” condition by varying the lubrication mechanism.

The experimental results show good agreement with the expectations provided by the theoretical model.

© 2008 Elsevier Ltd. All rights reserved.

---

## 1. Introduction

The “gear rattle” phenomenon is a research topic of great interest for the NVH (noise, vibration and harshness) automotive sector and concerns driveline noise and vibrations from the manual gear boxes. It is due to the internal combustion engine variable torque that causes impacts and rebounds, and consequently noise, between the teeth of the unloaded gear pairs of the gear box, due to the unavoidable presence of backlashes.

This inconvenience is, at present, largely studied by car manufacturers because it involves aspects of acoustic comfort inside and outside vehicles and represents an important factor in the highly competitive car market.

Today, small lightweight engines (often diesel engines with 3 cylinders), with more marked torque irregularities compared with engines adopted in past years, are very widespread, particularly in city cars.

---

\*Corresponding author. Tel.: +39 0817683292; fax: +39 0812394165.

E-mail address: [riccardo.russo@unina.it](mailto:riccardo.russo@unina.it) (R. Russo).

For this reason, new attention has been focused on investigating how a “noise free” driveline can be produced, attenuating all the undesired vibro-acoustic effects from the transmission components.

Previous papers [1,2] have proposed theoretical models that describe gear rattle in automotive transmissions.

Many theoretical investigations have been recently conducted which develop several aspects that may influence the phenomenon and offer various solutions to the problem [3–5]. Experimental analyses available in the literature are based on the measurement of the noise induced by the impacts, adopting airborne sound pressure meters. Often, in order to correlate the noise with the vibrations, the investigations also include measurement of the entire gear box vibrations (using accelerometers) [3,6–8]. These techniques are widely used especially in the car industry because they can compare different gear boxes or test various mechanical remedies on a single gear box. Considering that a vibro-acoustic disturbance propagates inside the vehicle through the structural way (chassis, gear box) as well as by the air, the above techniques can only give valid information when the solutions of the problem are compared by referring to the same gear box and the same vehicle. The experiments on the vehicle are therefore more useful for studying the effects rather than analysing the causes of the rattle phenomenon.

The remedies adopted in order to attenuate gear rattle may be divided into two categories, those outside and those inside the gear box. Devices such as multistaged clutches and dual-mass flywheels are typical external remedies. Internal measures to reduce rattle involve the design of the geometrical parameters of gears subject to impact load as well as the correct choice of lubricants and lubrication devices [5,8–10].

In the present paper, an experimental analysis isolating the influence of the lubricant on the gear rattle phenomenon is described.

The measurement methodology is based on the relative angular motion acquisition of the two wheels of a gear pair by means of two high resolution encoders in order to evaluate the vibrations due to the tooth impacts responsible for the acoustic disturbances.

## 2. The theoretical model

The investigation has been conducted in order to verify a theoretical model, already developed by the authors [9], that accounts for the oil squeeze effect between the gear teeth during the no-contact phases.

The model follows one of the classic approaches to gear rattle modelling. It consists of a lumped parameter one dof model representing the driven wheel mass that is forced to vibrate by the driving wheel motion.

In Fig. 1 the physical model of the gear pair is shown in three meshing configurations. The gear 1 represents the driving wheel.

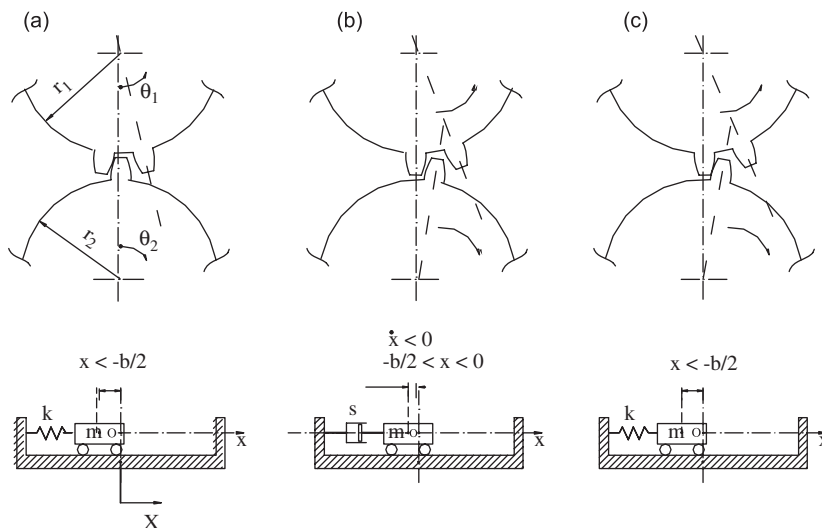


Fig. 1. Scheme of the one dof physical model of the gear pair: (a) contact, (b) separation, and (c) contact.

When the teeth are in contact (cases a and c), the interaction is expressed by an elastic force  $Kx$ , and, during the approach phase when the teeth are separated through an oil layer (case b), the oil squeeze effect gives a nonlinear damping force  $S\dot{x}$ . The contacts can occur either on the driving or on the driven side of the teeth.

Denoting with  $\Delta\theta$  the relative angular displacement between the gears

$$\Delta\vartheta = \vartheta_2 - \vartheta_1 \frac{r_1}{r_2} \tag{1}$$

the relative motion equation of the gear pair can be written as

$$-I_2\Delta\ddot{\vartheta} + F_c[\vartheta_1, \Delta\vartheta, \Delta\dot{\vartheta}]r_2 - T_b = I_2\ddot{\vartheta}_1 \frac{r_1}{r_2} \tag{2}$$

with

$$F_c(\vartheta_1, \Delta\vartheta, \Delta\dot{\vartheta}) = \begin{cases} K(\vartheta_1)r_2\Delta\vartheta & \text{if } |r_2\Delta\vartheta| \geq b \\ S(\Delta\vartheta)r_2\Delta\dot{\vartheta} & \text{if } |r_2\Delta\vartheta| \leq (b - h_{\min}) \\ S_{\max}r_2\Delta\dot{\vartheta} & \text{if } (b - h_{\min}) < |r_2\Delta\vartheta| < b \end{cases} \tag{3}$$

where  $I_2$  represents the driven gear moment of inertia,  $b$  is the backlash, and  $h_{\min}$  is a constant term representing the film thickness of the oil layer that remains adsorbed to the tooth surface during the contact phase.  $S_{\max} = S(h_{\min})$  is the saturation value of the squeeze damping coefficient.

Moreover, the resisting actions in the bearings supporting the unladen gear idle on its shaft are represented by a constant drag torque  $T_b$ .

Finally the compliance of the primary shaft is ignored and the system is driven by  $\vartheta_1(t)$ .

The genesis of the aforementioned stiffness  $K(\vartheta_1)$  and damping  $S(\Delta\vartheta)$  coefficients of the interaction forces  $F_c(\vartheta_1, \Delta\vartheta, \Delta\dot{\vartheta})$  has been discussed in previous papers [4,9–11].

With reference to an helical involute gear pair, the contact stiffness  $K(\vartheta_1)$  is given by the sum of the contributes due to the  $n$  tooth pairs that are in contact at the same time.

This stiffness, for a given gear pair, is function of the position of the driving gear during the meshing. The stiffness is consequently the sum of  $n$  periodic functions shifted each other of a transverse base pitch  $\Theta_p$ . The  $i$ -th function  $K_i(\vartheta_1)$  has the expression

$$K_i(\vartheta_1) = k_p \exp\left(C_a \left| \frac{\vartheta_1 - \varepsilon \Theta_p / 2}{1.125 \varepsilon_x \Theta_p} \right|^3\right) \tag{4}$$

where  $\varepsilon$  and  $\varepsilon_x$  are the total contact ratio and the transverse contact ratio, respectively, and  $\Theta_p$  is the transverse base pitch. The term  $k_p$  indicates the stiffness at the pitch point, that depends on the tooth parameters along with the  $C_a$  coefficient. These terms are detailed in Ref. [11].

With reference to a single tooth pair meshing near the pitch point, the oil damping term  $S(\Delta\vartheta)$  has been modelled under the following tribological assumptions:

- the teeth are rigid cylindrically shaped bodies whose axes are parallel to the gear axis;
- the radius of each cylinder is assumed to be the involute radius at the pitch point;
- the cylinders approach each other without any slip velocity (the oil squeeze effect is predominant);
- the fluid viscosity is assumed to be constant.

The analytical expression of the damping coefficient is given by [9]

$$S(x) = -3R^{3/2}\mu Z \frac{\left[ a(a^2 - Rx)\sqrt{Rx} + (a^2 + Rx)^2 \arctan\left(\frac{a}{\sqrt{Rx}}\right) \right]}{x^{3/2}(a^2 + Rx)^2} \tag{5}$$

where

$$x = \begin{cases} b - \Delta \vartheta r_2 & \text{if } \Delta \dot{\vartheta} > 0 \\ b + \Delta \vartheta r_2 & \text{if } \Delta \dot{\vartheta} < 0 \end{cases}$$

in which  $\mu$  is the absolute viscosity,  $Z$  indicates the axial width of the gear pair,  $R$  is the relative curvature radius of the teeth, and  $a$  denotes the semi-length of the oil film along the tooth surfaces related to the lubrication conditions.

### 3. The experimental test rig and measurement methodology

The experimental test rig (Fig. 2) comprises a single helical gear pair of an automotive gear box. Each wheel is splined to a shaft by a locking device and the primary shaft of the rig is moved by a speed controlled brushless motor.

The maximum output torque of the brushless motor is equal to 2.2 Nm and its speed controller, interfaced with a computer, enables suitable speed time histories to be developed.

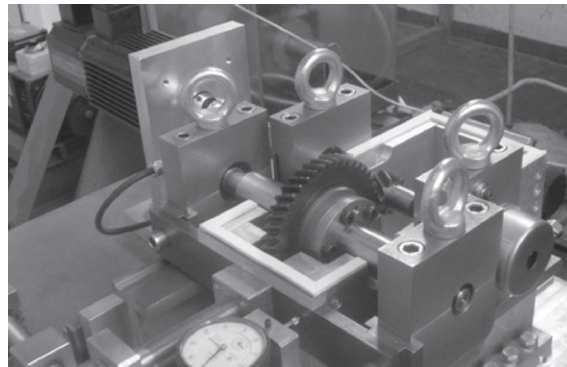
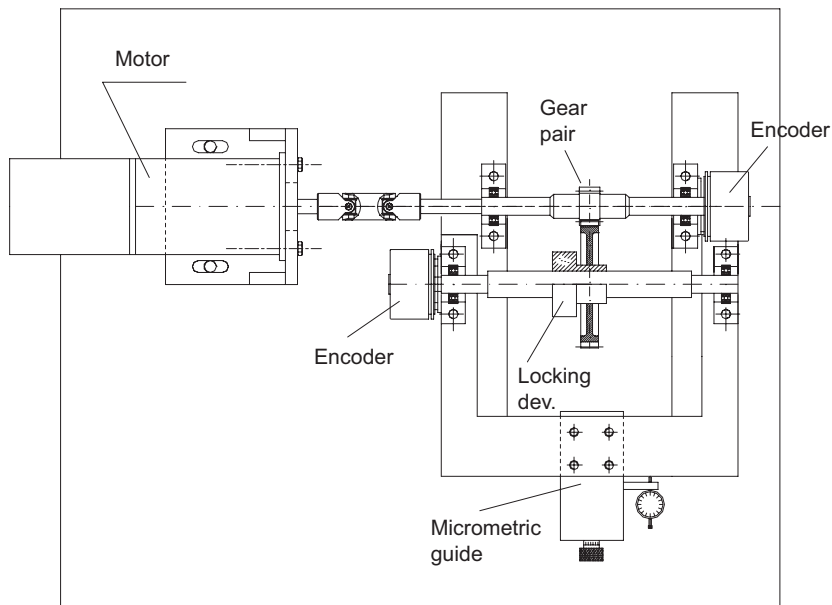


Fig. 2. The experimental test rig.

Apart from the resistant torque due to the drag forces exerted by the bearings, no external load is applied to the secondary shaft and the test rig therefore simulates an idle operating condition.

By using a micrometric linear guide connected to a small chassis supporting the secondary shaft, the value of the gear backlash can be modified by varying the wheel axes distance.

The comparison with the theoretical results must be conducted through an analysis of the time histories of the relative angular motion.

To do this, two incremental encoders (Baumer electric: 10 000 pulses/rev on each channel) have been fixed to the end of the two shafts. A counter/timer data acquisition board (NI 6802: 8 I/O channels, 32 bit), installed on a personal computer and programmed in N.I. LabView environment, performs a buffered reading of the signals from the two encoders. The simultaneity of the readings is guaranteed from a 10 kHz trigger realized using one of the output channels of the counter/timer board. The buffers of measure are transmitted, via DMA, to the computer for processing and storage on files.

The test rig is also equipped with an alloy tank posed below the gear pair containing the lubricant oil for the tests in the different lubrication conditions.

By virtue of a quadrature detection, each encoder provides a resolution of 40 000 pulses/rev (1.57e-4 rad).

As for the gear pairs under examination  $r_2$  is greater than  $r_1$ , the relative rotation in Eq. (1), is measured in the present analysis by combining the two absolute rotations in this way:

$$\Delta\vartheta^*(t) = \vartheta_1(t) - \vartheta_2(t) \frac{r_2}{r_1} = -\Delta\vartheta(t) \frac{r_2}{r_1} \tag{6}$$

A better resolution in the angular motion measurements can be so obtained.

During determination of the value of angular backlash between the teeth, being the secondary wheel firm, the uncertainty of the measure, assuming a distribution of probability uniform inside the resolution, is given by

$$U_{\Delta\Theta} = \frac{1}{2\sqrt{3}} \left( \frac{2\pi}{40\,000} \right) = 4.5E - 05 \tag{7}$$

Under dynamic conditions, on the other hand, the combined uncertainty in the measure of the relative rotation, still assuming uniform distribution inside the resolution, is given by

$$U_{\Delta\Theta} = \frac{1}{2\sqrt{3}} \left( \frac{2\pi}{40\,000} \right) \sqrt{1 + \left( \frac{z_2}{z_1} \right)^2} \tag{8}$$

Table 1 presents the value of the uncertainty type for the two different gear pairs used in the tests.

The angular backlash, i.e., the angular rotation of the primary wheel corresponding to the recovery of the gap between one of its teeth and the two teeth of the secondary wheel, not only depends on the constructive parameters of the wheels themselves, but also on the actual value of the distance between the gear axes. Depending on the values of the above constructive and operating parameters, the angular backlash ranges from 0.01 to 0.07 rad. In every case, therefore, the uncertainty of measure is always at least two orders of magnitude smaller than the backlash to be measured.

In order to illustrate measurement quality, Fig. 3 shows the angular relative motion as a function of the absolute motion of the primary gear. The figure refers to the first speed pair in no-rattle condition. The pair is characterized by 11 teeth on the primary and 43 on the secondary gear. On the primary gear, a constant speed motion (about 250 rev/min) is imposed in order to establish a permanent contact between the flanks of the two

Table 1  
Measurement uncertainty.

	$Z_2$	$Z_1$	$U_{\Delta\Theta}$ (rad)
I	43	11	1.8E-04
II	41	19	1.1E-04

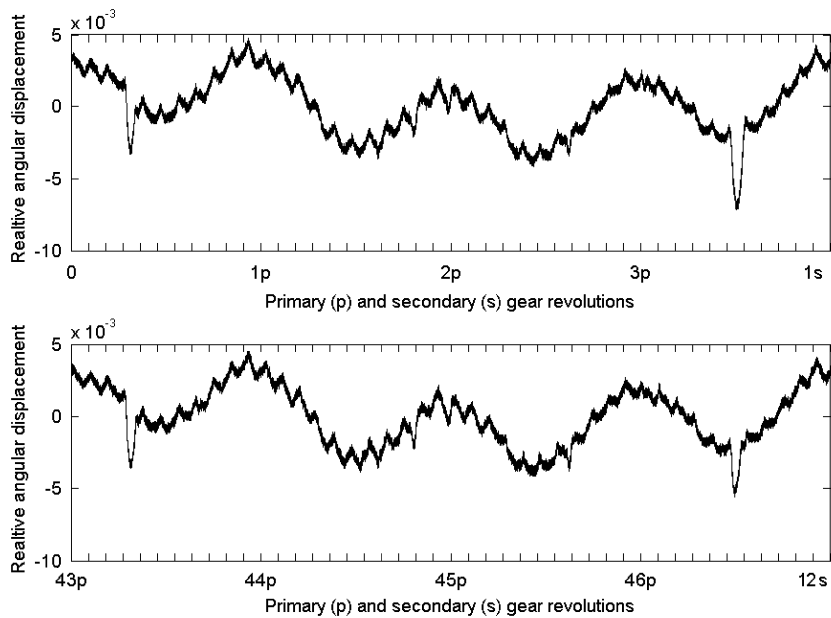


Fig. 3. A typical angular relative motion acquisition in no-rattle conditions.

gears. In the abscissa, four revolutions of the primary gear are reported: those numbered 1–4 (top diagram) and those numbered 44–47 (bottom diagram). The two diagrams are then compared with the meshing of the same pairs of teeth on the two gears and, as expected, are practically coincident.

By examining the diagrams, a high frequency vibration can be seen whose period is equal to  $1p/z_1$  ( $z_1 = 11$ ), as illustrated by the axis ticks. This frequency is attributable to the gear meshing.

The presence of two periodical modulations due to the eccentricities of both the wheels can also be noted.

The primary wheel has an eccentricity whose period is equal to  $1p$ , due to its revolution. The other periodicity, corresponding to the secondary wheel eccentricity, has a period equal to  $3.9p$  (i.e.,  $1s$ ) due to the particular transmission ratio  $\varepsilon = 3.9$ , and it is less evident in the diagram compared with the previous one. For the pair being examined, the eccentricity of the pinion (driving gear) is easily recognizable in the figure because its amplitude is the greater one (about  $3e^{-3}$  rad).

Moreover, the figure shows the presence of a spike in the contact phase, occurring two times during a revolution of the driven (secondary) gear. It indicates a defect in two teeth on this wheel at abscissa  $3/11p$  (or  $3/43s$ ) and  $38/11p$  (or  $38/43s$ ), respectively. In this context, it is very interesting to note the good stability of the experimental measure which can be seen by comparing the relative motion curves referred to the meshing of the same teeth pairs on the two gears that show a perfect superimposition of the aforementioned tooth defects.

All the effects described in this paragraph, due to the tooth characteristics, have been found in all the experimental acquisitions and their magnitude varies depending on the different gear pairs.

Fig. 4 shows an example of the acquisition of the first speed relative motion, referred to a classical gear rattle condition, in which two fluctuation bands can be seen. Within these fluctuation bands, two types of meshing contacts between the teeth flanks take place; in particular, in the bottom band (B side) the driving gear teeth push on the driven gear ones and vice versa in the top band (A side).

Recalling Fig. 3, it can be seen that the contact occurring within those fluctuation bands takes into account for all those effects caused by: errors in the teeth machining (gear meshing), errors in the mounting (wheel eccentricity), and teeth splitting defects.

Such fluctuation bands for the specific gear pair that is under examination (first speed) have an overall extension of about  $0.015$  rad, corresponding to the contact fluctuations measurements shown in Fig. 3.

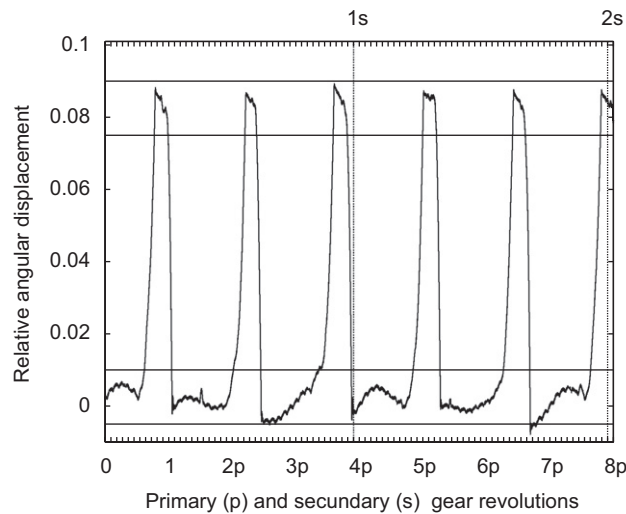


Fig. 4. A typical angular relative motion acquisition in the event of gear rattle.

Table 2  
The gear pair parameters.

Driving	$Z$	$b$	$\phi$	$\varepsilon$	Driven	$Z$	$b$	$\phi$
I	11	17	26.477	3.909	I	43	13.8	103.501
II	19	13.5	41.173	2.157	II	41	12.8	88.847

#### 4. Description of tests

Using the same apparatus, the first and the second gear pairs of an automotive gear box were tested by varying both the lubrication conditions and the backlashes (varying the distance between the wheels axes) for each pair.

The characteristic parameters of the two gear pairs under examination are reported in the following Table 2, indicated with  $z = n^\circ$  of teeth;  $b =$  teeth width (mm);  $\phi =$  pitch diameter (mm);  $\varepsilon =$  transmission ratio.

The system has been characterized calculating the flexural critical speed, by a lumped mass model, giving so a value of about 21 000 rev/min (350 Hz). The driven wheel being unloaded, its shaft can be considered torsionally rigid and so, referring to the physical scheme of Fig. 1, the only possible resonance regards the meshing stiffness during the contact of the teeth. For this system the natural frequency has been estimated in about 3400 Hz.

##### 4.1. Backlash determination

For every wheel pair and every value of the distance between the axes, a measurement of the operating backlash is preliminarily effected. This measurement is obtained with a motion law at the primary wheel that effects a small oscillation around an angular position. The backlash between the teeth of the primary wheel and the two teeth of the driven wheel is therefore alternatively recovered along the two directions.

The difference between the maximum and the minimum ordinate values of the oscillations acquired in this way is associated to the value of the backlash for the gear pair under examination. As shown above, the circumferential backlash for each pair may not be constant when varying the meshing teeth in contact because of possible eccentricities due to the assembly (run-out) or working errors. For this reason, by repeating the measure for a great number of angular positions, i.e., different pairs of meshing teeth, a statistic estimation of the mean operating backlash has been obtained.



Table 3  
Oil parameters.

Oil viscosity (40 °C)	156.5 cSt
Oil viscosity (100 °C)	15.7 cSt
Oil density	890 kg m <sup>-3</sup>

#### 4.2. Gear rattle tests

The tests have been constructed to investigate the influence of the variation of the lubrication conditions and, in particular, of the oil amount interposed between the teeth. The three lubrication mechanisms adopted are, respectively:

- “dry conditions” obtained by cleaning the gear pair with a suitable solvent;
- “boundary lubrication” obtained by applying a thin film of oil to the flanks of the teeth;
- “oil jet lubrication”, obtained by pumping a jet of oil into the meshing zone.

The oil used in the tests is a typical transmission lubricant (Eurocube eplus 5: SAE 80 W/90), the properties of which are given in Table 3:

In the tests, for an oil temperature of approximately 20 °C, a viscosity value ( $\mu$ ) of 0.5 Pas has been estimated.

In order to examine the dynamic behaviour of a gear pair in operative conditions corresponding to low average speed values, the following law for the motor speed has been adopted:

$$\omega(t) = \dot{\vartheta}_1(t) = \Omega_m + \Delta\Omega \sin(2\pi ft) \quad (9)$$

where  $\Omega_m$  is the speed mean value;  $\Delta\Omega$  and  $f$  are the amplitude and the frequency of the speed fluctuation respectively. The  $\Omega_m$  maximum value adopted in the tests is 500 rev/min; the values of the speed amplitude fluctuation were typically in the range 10–20% of the speed mean value. The values of the fluctuations frequencies were 4, 8, and 16 Hz.

These fluctuations frequencies with their significant harmonics, and the gear meshing frequencies, are in every case lower than the aforementioned calculated critical frequencies.

### 5. Experimental results

Fig. 5 shows, as an example, the time history acquired during a backlash determination concerning the first speed gear pair. The absolute motion of the two wheels and the relative angular displacement can be seen in the figure. The driven wheel, in particular, instead of being motionless, makes some small movements as a result of the impacts with the teeth of the primary wheel. The figure also shows good resolution and repeatability of the measurements.

In Fig. 6, the mean value over 90 measurements of the angular backlash as a function of the axis to axis distance is reported for the gear pairs under investigation. In Fig. 7, the circumferential backlash values obtained starting from the previous angular mean values multiplied by the driving wheel radii of the gear pairs indicated in Table 2 have been also reported.

The distance between the wheels axes ranges from 65.0 to 66.0 mm where 65 mm is the design value prescribed for such gear pairs.

In Figs. 8 and 9, some typical time histories of the relative angular motion of the gears are reported. For both figures, the operating parameter values are  $\Omega_m = 52.36 \text{ s}^{-1}$  (500 rev/min),  $\Delta\Omega = 10.47 \text{ s}^{-1}$  (20% of  $\Omega_m$ ), and  $f = 16 \text{ Hz}$ , and the lubrication mechanism are (a) dry contact and (b) oil jet lubrication. Fig. 8 refers to the first speed gear pair and Fig. 9 to the second speed gear pair. In order to emphasize the gear rattle phenomenon, the distance between the axes has been increased to a value of 66.0 mm for the first speed and



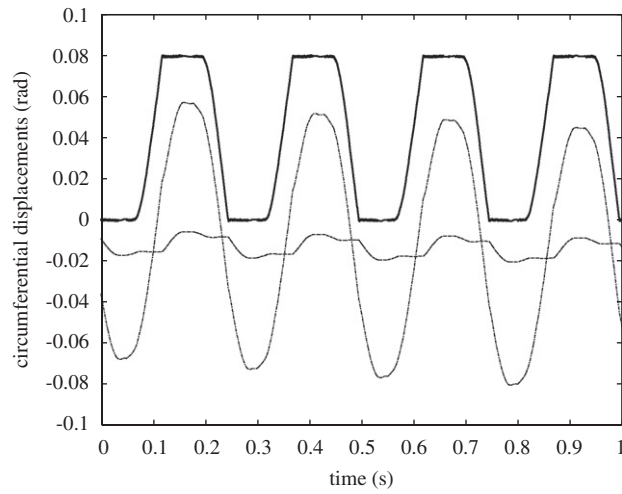


Fig. 5. A typical backlash acquisition. (---: primary gear absolute motion; ·····: secondary gear absolute motion; —: relative angular motion).

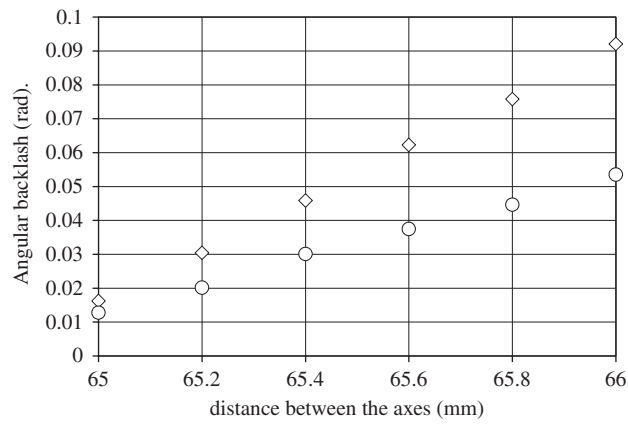


Fig. 6. Angular backlash vs. axis to axis distance. (◇): first speed; (○): second speed.

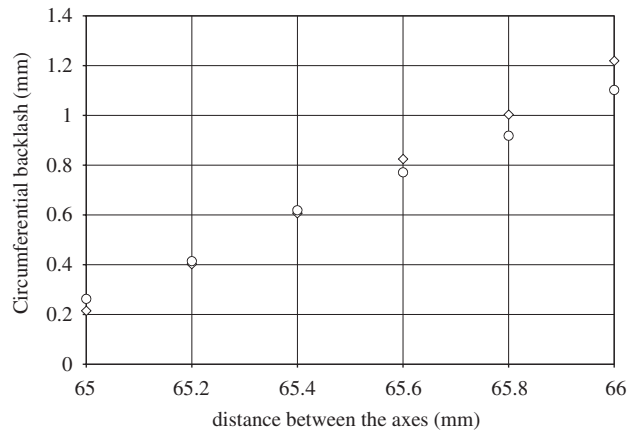


Fig. 7. Circumferential backlash vs. axis to axis distance for the first (◇) and second (○) speed.

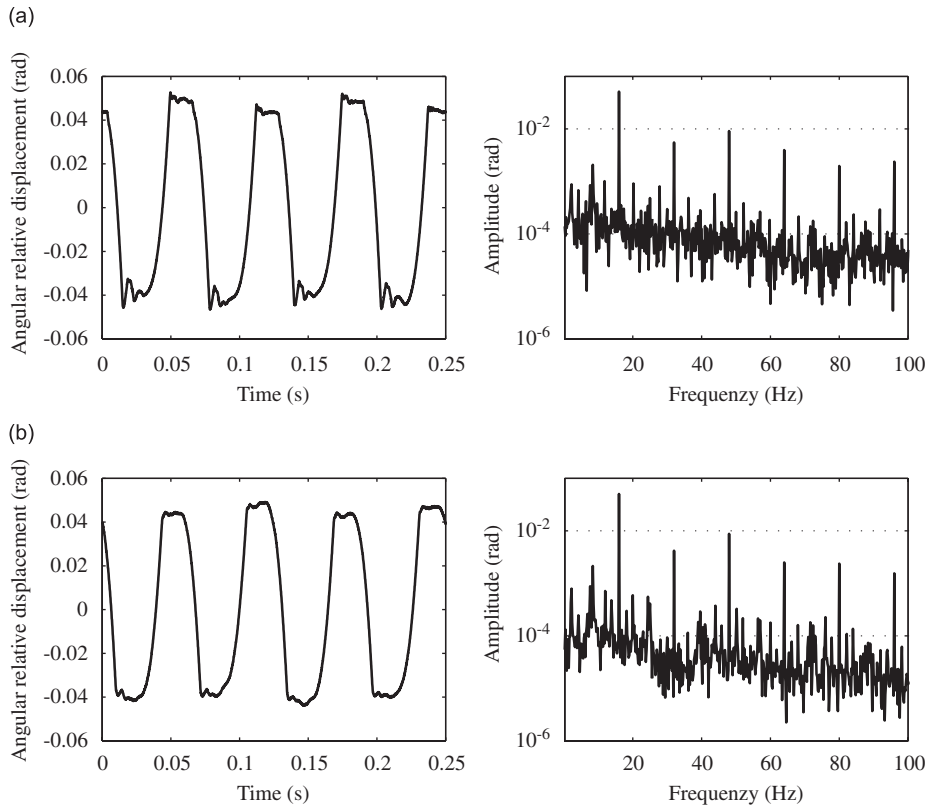


Fig. 8. Experimental results for the first speed varying the lubrication mechanism: (a) dry contact; (b) oil jet lubrication. Operating parameters:  $\Omega_m = 52.36 \text{ s}^{-1}$ ;  $\Delta\Omega = 20\%$ ;  $f = 16 \text{ Hz}$ .

65.6 mm for the second speed. For the above distances, the estimated angular backlash values are 0.092 (first speed in Fig. 8) and 0.038 rad (second speed in Fig. 9).

In the relative motion diagrams in Figs. 8 and 9, the classic situations of bilateral hits (“double sided impacts”) can be noted. In dry contact conditions, hits and rebound between the flanks of the tooth are evident especially in the phase of contact in which the driving wheel pushes the driven one (in the bottom side of the diagrams). In oil jet lubrication conditions, a reduction in the hits between the opposite flanks of the teeth is observed and corresponds to a more favorable rattling condition.

Looking at the FFT diagrams, a reduction in the amplitude of all the harmonic components when passing from dry conditions to oil jet lubrication conditions can be seen.

This circumstance clarifies the meaning of a “gear rattle index” (IGR) that has been defined here and adopted in order to discriminate, in an objective way, between the different vibro-acoustic behaviours caused by different lubrication conditions. The above IGR has been calculated as the value of the following integral:

$$IGR = \int_{20}^{5000} |\Delta\vartheta^*(\omega)| d\omega \tag{10}$$

where  $|\Delta\vartheta^*(\omega)|$  is the relative motion Fourier transform magnitude.

In Fig. 10, for the first speed gear pair, this index has been reported as a function of the distance between the axes (i.e., the circumferential backlash) in the two different lubrication mechanisms: *boundary* and *oil jet* lubrication.

As can be observed in the experimental results, the indexes grow as the backlash increases and this tendency is confirmed for all the lubrication conditions.

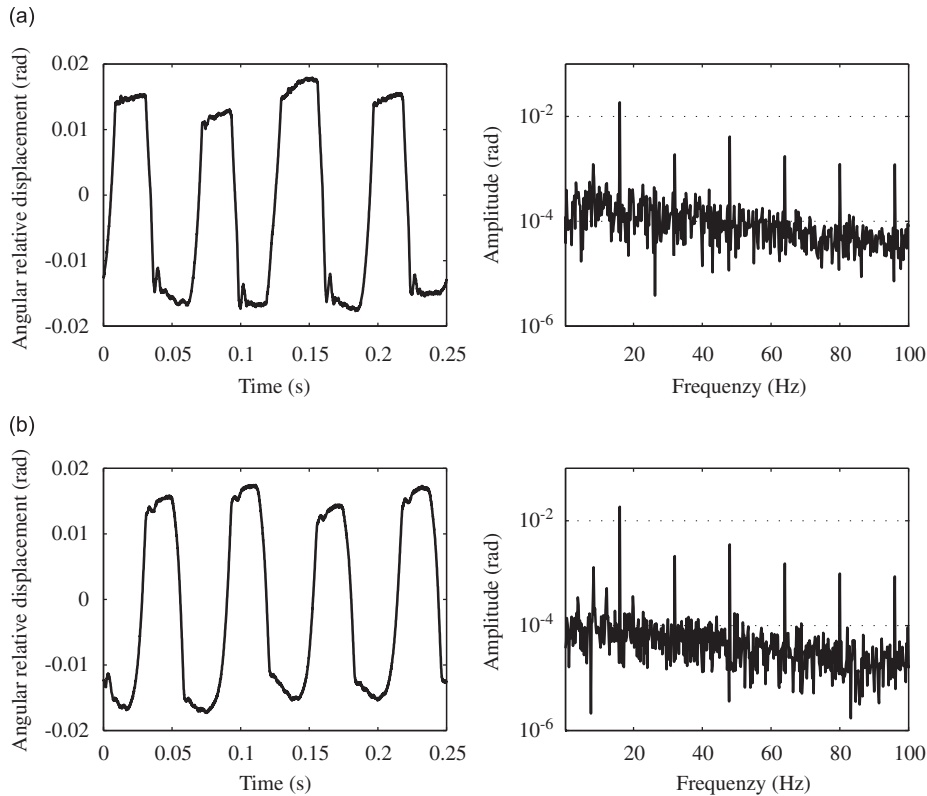


Fig. 9. Experimental results for the second speed varying the lubrication mechanism: (a) dry contact; (b) oil jet lubrication. Operating parameters:  $\Omega_m = 52.36 \text{ s}^{-1}$ ;  $\Delta\Omega = 20\%$ ;  $f = 16 \text{ Hz}$ .

Once again, for the second speed, in Fig. 11, the gear rattle index has been reported in the three different lubrication mechanisms: *dry contact*, *boundary*, and *oil jet* lubrication.

By examining the diagrams, it can be noted that generally the indexes values slightly decrease, as expected, passing from the *dry* to the *boundary* condition that represents a poor lubrication mechanism while the decrease appears more appreciable in the *oil jet* condition where the amount of lubricant increases.

The IGR index therefore shows, with few exceptions, a fairly good capacity in discriminating the different lubrication conditions adopted in the tests.

## 6. Theoretical–experimental correlation

In order to validate the theoretical model, previously developed by the authors, some comparisons have been conducted between the simulation results and the experimental data and a reasonable agreement has been generally observed.

In particular, a theoretical–experimental correlation has been performed by using the aforementioned gear rattle index IGR and varying the circumferential backlash for the different tested lubrication regimes.

The dynamic operative conditions adopted for the comparisons are those corresponding to the following test parameters: a mean velocity of  $\Omega_m = 52.36 \text{ s}^{-1}$ , a speed fluctuation of 20% and a frequency of 16 Hz.

In the theoretical simulations, the value of the oil viscosity has been calculated starting from the oil temperature measured by a sensor that in the “C” condition has been immersed in the lubricant flux close to the meshing teeth zone. With regard to the resistant torque ( $T_b$ ) in the motion equations due to the bearings,

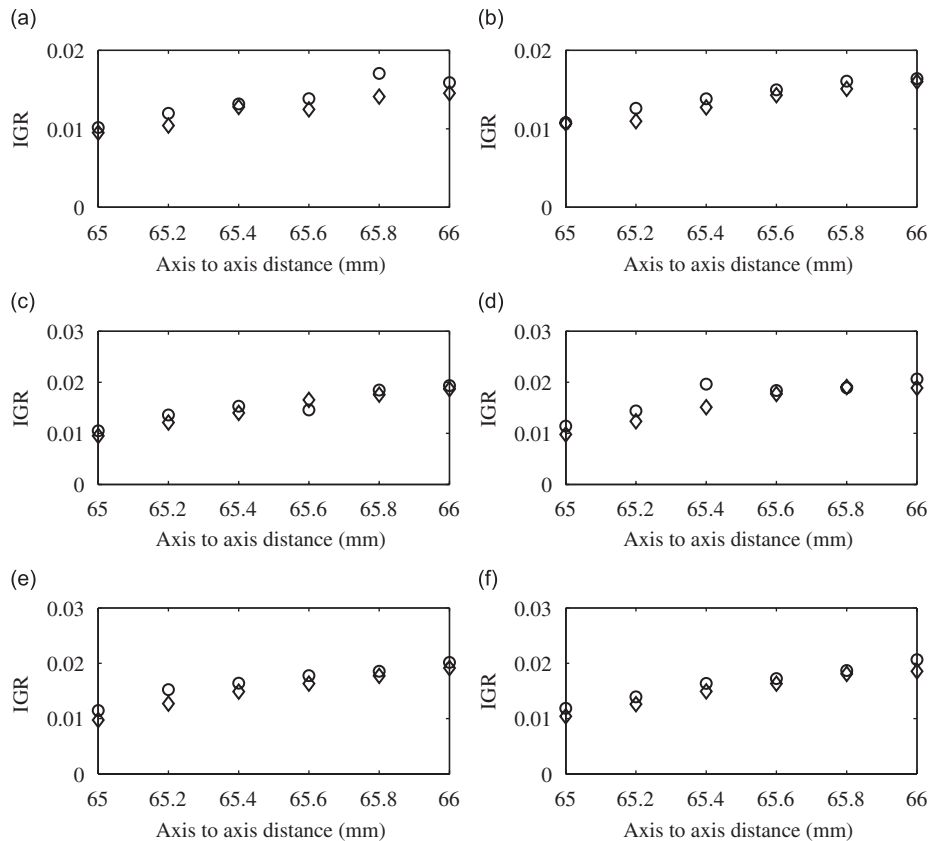


Fig. 10. Experimental results for the first speed gear pair: IGR vs. axis to axis distance. (o): boundary lubrication; ( $\diamond$ ): oil jet lubrication. Operating parameters:  $\Omega_m = 52.36 \text{ s}^{-1}$ ; (a)  $\Delta\Omega = 10\%$ ,  $f = 4$  Hz; (b)  $\Delta\Omega = 20\%$ ,  $f = 4$  Hz; (c)  $\Delta\Omega = 10\%$ ,  $f = 8$  Hz; (d)  $\Delta\Omega = 20\%$ ,  $f = 8$  Hz; (e)  $\Delta\Omega = 10\%$ ,  $f = 16$  Hz; (f)  $\Delta\Omega = 20\%$ ,  $f = 16$  Hz.

its value depends on a number of operating parameters such as kind and size of bearings, velocity, oil viscosity, lubrication mechanism, etc. For a first estimation, the formula reported in Ref. [12] concerning bearing losses has been adopted.

Special attention has been paid to the estimation of parameters that are difficult to evaluate “a priori” in the mathematical model such as the oil film half-extension in the gap between the teeth flanks (the  $a$  term in Eq. (5)). In order to find a correct value for this parameter, a comparison between the theoretical and experimental FFTs spectra of the gear relative motion has been adopted. As a result, the values of the aforementioned parameter were  $a = 0.07\text{--}0.1$  mm in the “B” cases (*boundary* lubrication) and  $a = 1$  mm for the “C” cases (*oil jet* lubrication).

Regarding the value of the backlash (the  $b$  term in Eq. (3)), in the theoretical model for every axis to axis distance, the mean value has been adopted thus neglecting the periodic fluctuations of this parameter (see Fig. 3) since their amplitudes for the second gear pair were very small compared with the backlash.

With regard to the experimental-theoretical correlation in terms of gear index, for the lubricated cases “B” and “C”, the results showed qualitatively good agreement independently of the gear pair considered. In some cases, particularly for the smaller backlash values, the comparisons also give quantitatively good agreement as can be seen in the results reported in Fig. 12 for the second speed.

As far as the “A” dry condition case is concerned, the correlation with the theoretical model provided results that were quantitatively not in agreement with the experimental data but qualitatively confirmed the experimental trend for both the considered gear pairs. In Fig. 13, the theoretical–experimental correlation in

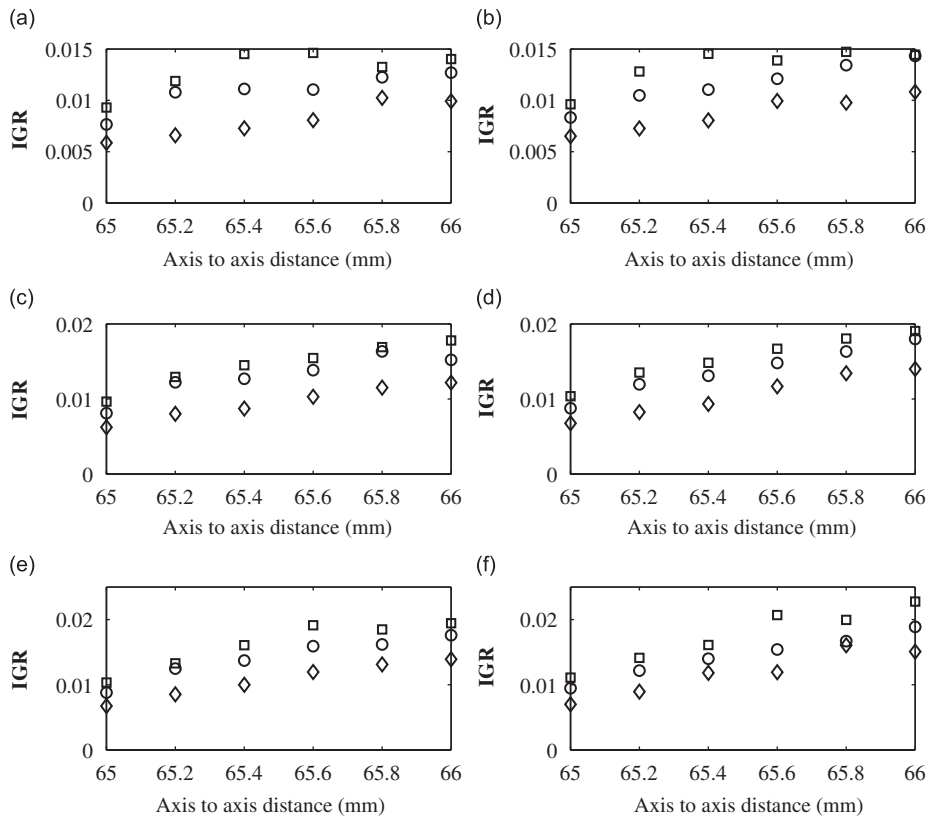


Fig. 11. Experimental results for the second speed gear pair: IGR vs. axis to axis distance. ( $\square$ ): dry contact; (o): boundary lubrication; ( $\diamond$ ): oil jet lubrication. Operating parameters:  $\Omega_m = 52.36 \text{ s}^{-1}$ ; (a)  $\Delta\Omega = 10\%$ ,  $f = 4 \text{ Hz}$ ; (b)  $\Delta\Omega = 20\%$ ,  $f = 4 \text{ Hz}$ ; (c)  $\Delta\Omega = 10\%$ ,  $f = 8 \text{ Hz}$ ; (d)  $\Delta\Omega = 20\%$ ,  $f = 8 \text{ Hz}$ ; (e)  $\Delta\Omega = 10\%$ ,  $f = 16 \text{ Hz}$ ; (f)  $\Delta\Omega = 20\%$ ,  $f = 16 \text{ Hz}$ .

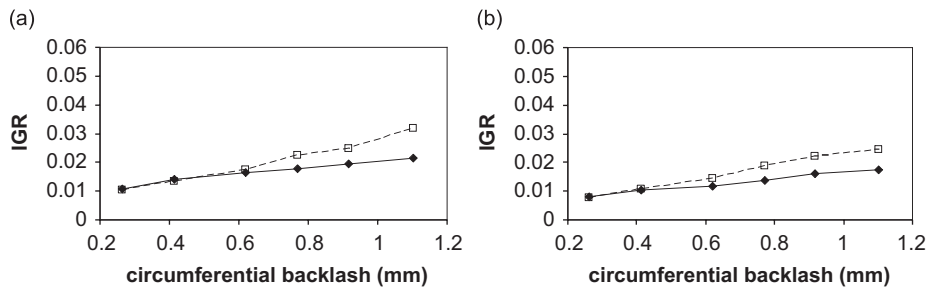


Fig. 12. Theoretical–experimental comparison for the second speed: (a) *boundary* lubrication; (b) *oil jet* lubrication. (– $\diamond$ – experimental data; – $\square$ – theoretical data.)

the “dry” condition for the second gear pair is reported. In this case, the theoretical model gave, in term of indexes, values that were higher than the experimental ones, thus overestimating the rattle phenomenon. This fact is certainly due to the absence of a dissipative term in the motion equations accounting for the sliding friction during the “dry” meshing phase. It is important to underline that the “dry” contact, representing a condition that is very different from the normal operative conditions of a transmission gear pair, has only been used in the analysis as a datum point for the experimental comparisons. For this reason, the theoretical model developed by the authors does not account for the dissipative term mentioned above.

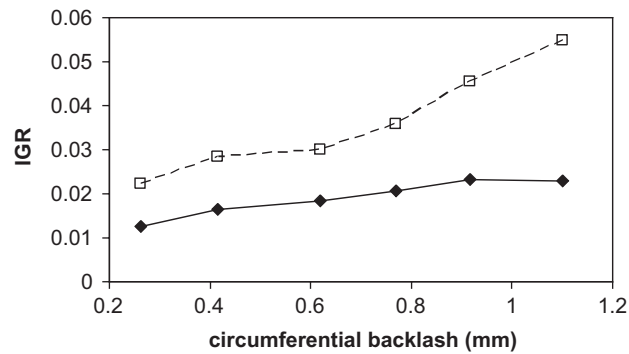


Fig. 13. Theoretical–experimental comparison for the second speed in the “dry” condition. (–◆– experimental data; –□– theoretical data.)

## 7. Conclusions

In the present paper, the results of a series of experiments acquired on a test rig developed in order to simulate the behaviour of an helical gear pair under the condition of “idle gear rattle” by varying the lubrication conditions have been reported and subsequently compared with the theoretical expectations.

In order to discriminate the different behaviours regarding the gear rattle phenomenon, an index has been proposed in the analysis. This index can be useful when evaluating the different rattle levels.

The theoretical model adopted, previously developed by the authors, accounts for the squeeze effect of the oil between the gear teeth in order to better approximate the damping due to the lubricant during the no-contact phase.

An examination of the experimental results when varying the lubrication mechanism, demonstrated the positive influence due to this oil damping factor in reducing the impacts and, in general, rattle vibration. This effect is independent of the operating parameters as well as the speed and frequencies of the speed fluctuations. Moreover, this behaviour also seems to be independent of the backlash between the teeth.

With regard to the theoretical validation, the conducted experimental investigation shows qualitatively good agreement with the numerical simulations obtained when adopting a one dof model.

The present analysis therefore reinforces the belief of some researchers, endorsed by the authors, that the damping action exerted by the oil lubricant between the gear meshing teeth cannot be neglected when modelling the gear rattle.

Theoretical models that neglect this oil damping effect during the separation phase lead to an overestimation of the gear rattle phenomenon, unless an overall dumping term, empirically evaluated, is considered.

## References

- [1] R. Singh, H. Xie, R.J. Comparin, Analysis of automotive neutral gear rattle, *Journal of sound and vibration* 131 (2) (1989) 177–196.
- [2] Y. Wang, R. Manoj, W.J. Zhao, Gear rattle modeling and analysis for automotive manual transmissions, *Proceedings of ImechE—Part D, Journal of Automobile Engineering* 215 (2001) 241–258.
- [3] S.N. Dogan, J. Ryborz, B. Bertsche, Design of low-noise manual automotive transmissions, *Proceedings of IMechE—Part K, Journal of Multi-body Dynamics* 220 (2006) 79–95.
- [4] R. Brancati, E. Rocca, R. Russo, An analysis of the automotive driveline dynamic behaviour focusing on the influence of the oil squeeze effect on the idle rattle phenomenon, *Journal of Sound and Vibration* 303 (3–5) (2007) 858–872.
- [5] S. Theodossiades, O. Tangasawi, H. Rahnejat, Gear teeth impacts in hydrodynamic conjunctions promoting idle gear rattle, *Journal of Sound and Vibration* 303 (3–5) (2007) 632–658.
- [6] A. Forcelli, T. Pappalardo, C. Grasso, A new approach for objective measurements of transmission gear rattle noise, *2004 JSAE Annual Congress*, Yokohama, Japan, 19–21 May, 2004.
- [7] F. Sbarbati, C. Grasso, M. Martorelli, P. Liccardo, L. Tosato, M. Uberti, M. Malusardi, Gear rattle optimization, *FISITA 2004, World Automotive Congress*, Barcelona, Spain, 2004, pp. 23–27.
- [8] S. Theodossiades, O. Tangasawi, H. Rahnejat, Lightly loaded lubricated impacts: idle gear rattle, *Journal of Sound and Vibration* 308 (2007) 418–430.

- [9] R. Brancati, E. Rocca, R. Russo, A gear rattle model accounting for oil squeeze between the meshing gear teeth, *Proceedings of IMechE—Part D, Journal of Automobile Engineering* 219 (9) (2005) 1075–1083.
- [10] R. Brancati, E. Rocca, R. Russo, F. Timpone, Experimental test rig for the evaluation of oil squeeze effects between the impacting teeth of a meshing gear, *AITC-AIT 2006, 5th International Conference on Tribology*, Parma, Italy, ISBN: 978-88-902333-0-2, 2006.
- [11] Y. Cai, Simulation on the rotational vibration of helical gears in consideration of the tooth separation phenomenon (a new stiffness function of helical involute tooth pair), *Transactions of the ASME, Journal of Mechanical Design* 117 (1995) 460–469.
- [12] SKF-Bearing Catalogue, Copyright SKF 1999.